HCMV infection activates NLRP3 inflammasome by releasing mtDNA into cytosol in human THP-1 cells

Xi Xu
Wenzhou Medical University
Yutian Lu
Wenzhou Medical University
Kaizhao Huang
Children's Hospital of Wenzhou Medical University
Binhan Guo
Children's Hospital of Wenzhou Medical University
Yangyang Fang
Children's Hospital of Wenzhou Medical University
Meimei Lai
Children's Hospital of Wenzhou Medical University
Linhua Lan
Wenzhou Medical University
Ying Peng
Wenzhou Medical University
Xiaoqun Zheng (jszhengxq@163.com)
Wenzhou Medical University

Research Article

Keywords: Human Cytomegalovirus, Infection, NLRP3, mitochondria, mtDNA

Posted Date: March 1st, 2022

DOI: https://doi.org/10.21203/rs.3.rs-1313406/v1

HCMV infection activates NLRP3 inflammasome by releasing mtDNA into cytosol in human THP-1 cells

Xi Xu[1,2,3,4#], Yutian Lu[2,3,#], Kaizhao Huang[1,2,3], Binhan Guo[1,2,3], Yangyang Fang[1,2,3], Meimei Lai[1,2,3], Linhua Lan[2], Ying Peng[2,3], and Xiaoqun Zheng[1,2,3*]

Running title: HCMV infection activates NLRP3 inflammasome

[1]Department of Clinical Laboratory, the Second Affiliated Hospital and Yuying Children's Hospital of Wenzhou Medical University, Wenzhou, Zhejiang, China

[2]School of Laboratory Medicine and Life Science, Wenzhou Medical University, Wenzhou, Zhejiang, China

[3]The Key Laboratory of Laboratory Medicine, Ministry of Education, Wenzhou, Zhejiang, China

[4]Department of Clinical Laboratory, Wenzhou People's Hospital, The Third Clinical Institute Affiliated to Wenzhou Medical University, Wenzhou, China

#These authors contributed equally to this work.

[*]**Correspondence:**

Name: Xiaoqun Zheng

E-mail: jszhengxq@163.com

Phone number: 13906653839

Affiliation: Wenzhou Medical University

Postal address: Wenzhou Medical University, Wenzhou City, Zhejiang Province, China

Abstract

Human Cytomegalovirus (HCMV) infection of monocytes results in the production of inflammatory cytokine interleukin-1β (IL-1β). The objective of the study was to explore the mechanism behind the activation of inflammation. HCMV infection activated the NLRP3 inflammasome and enhanced the secretion of IL-1β in THP-1 cells. Besides, HCMV infection caused mitochondrial dysfunction, including excessive ROS production, decreased mitochondrial membrane potential, and increased mitochondrial fusion. Importantly, the infection reduced the expression of TFAM protein and the release of mitochondrial DNA into the cytoplasm, which may contribute to the activation of NLRP3 inflammasome. Collectively, our finding suggests that HCMV infection may activate NLRP3 inflammasome by releasing mtDNA into the cytosol in human THP-1 cells and provides novel insights into the innate immune response against HCMV infection.

Keywords: Human Cytomegalovirus; Infection; NLRP3; mitochondria; mtDNA

Background

Human cytomegalovirus (HCMV), an opportunistic pathogenic virus，can infect bone marrow monocytic lineage cells, causing severe diseases in immunocompromised populations [1, 2]. HCMV infection can evoke inflammatory

responses through the production of pro-inflammatory cytokines. It is thought that HCMV is associated with several diseases such as vascular disease, inflammatory bowel disease, and abnormal neurodevelopment in infants and children [3-6]. Thus，exploring the mechanism of HCMV-inducing inflammation, is important to pinpoint the role of HCMV in the etiology of these diseases.

The innate immune response is the first obstacle of pathogenic infection by microorganisms, aiming to prevent pathogen invasion by activating inflammasomes and releasing inflammatory factors [7]. Inflammasome, consisting of a pattern recognition receptor, an adaptor protein, and pro-caspase-1, can regulate the maturation and secretion of inflammatory cytokines to fight viruses [8]. The important sensor in inflammasome is the NLR family pyrin domain containing 3 (NLRP3) involved in some viral infections like the Ebola virus, Epstein-Barr virus, or influenza virus [9-11]. However, it is still less clear whether HCMV infection can activate the inflammasome in THP-1 monocytes

Mitochondria, a double-membrane structural organelle that produces ATP to maintain biological function, plays an important role in cellular energy metabolism and innate immune response [12-14]. Recent studies have shown that reactive oxygen species (ROS), mitochondrial dynamics, mtDNA leakage of the damaged mitochondria, and mitochondrial dysfunction are participants in mitochondrial regulation of innate immunity and inflammatory responses [15-18]. Whether HCMV infection impacts mitochondria in myeloid lineage (i.e., THP-1 cells) and whether mtDNA is involved in NLRP3 inflammasome activation remain largely unknown.

Results

HCMV infection causes mitochondrial dysfunction and mtDNA releasing into cytosol in THP-1 cells

We used sucrose gradient centrifugal-purified HCMV (MOI=5) to infect THP-1 cells. THP-1 cells were infected by HCMV Towne strain (Fig. 1A). In the infected THP-1 cells, the level of IE1 mRNA increased initially after infection but decreased over time, whereas the LUNA mRNA was detectable throughout infection and the expression of UL83 mRNA was not expressed.

Mitochondria are the target of viral attacks, and viral infections have a varying degree of effects on mitochondria [19, 20]. To examine the impact of HCMV infection on mitochondrial function, we measured ROS levels 48 hours after infection and found that HCMV infection significantly induced ROS production in THP-1 cells. (Fig. 1B). At the same time, mitochondrial membrane potential ($\Delta\Psi m$), which is important for mitochondrial homeostasis, was decreased after HCMV infection (Fig. 1C).

Mitochondrial dysfunction is manifested by the release of mtDNA [21]. Next, we analyzed the expression of TFAM (transcription factor A, mitochondrial), which binds to mtDNA, promoting its compaction and stabilization as well as replication and transcription [22]. The expression level of TFAM protein and mRNA in THP-1 cells was reduced upon HCMV infection (Fig. 1D-F). We also measured mtDNA amount in infected and uninfected THP-1 cells by qPCR. MtDNA copy number was reduced in

HCMV-infected cells compared with control cells (Fig. 1G). 2-fold increased the amount of the specific mtDNA fragment from the D-loop regulatory region in the cytosolic extract that was isolated from HCMV-infected cells compared with control cells, suggesting that mtDNA was released into the cytosol in HCMV-infected cells (Fig. 1H).

Together, our results indicate HCMV infection causes a dramatic increase in mtDNA damage in the infected cells.

HCMV infection interrupts mitochondrial dynamics in THP-1 cells

Mitochondrion is a dynamic organelle that undergoes continuous fission and fusion of the mitochondrial outer and inner membranes [23]. Mitochondrial morphology is tightly regulated by dynamic mitochondrial quality control mechanisms, including mitochondrial biogenesis, mitophagy, fusion, and fission [24]. Confocal and electron microscopy of HCMV-infected cells revealed significantly elongated and interconnected mitochondrial networks, consistent with a hyperfused phenotype (Fig. 2A-D). Accordingly, the protein levels of MFN1, OPA1 and OMA1, which are associated with mitochondrial fusion, were increased at 12 hpi (hours post-infection) and remained elevated through 72 hpi (Fig. 2E-H). Mitochondrial fusion is thought to be a defense mechanism regulated by mitochondrial fusion proteins MFN1, OMA1, and OPA1 [25]. OMA1 is a master regulator of mitochondrial fusion. MFN1 is the key protein for mitochondrial outer membrane fusion, and OPA1 mediates the inner membrane fusion [26]. DRP1 controls fission [27].

HCMV infection significantly activates NLRP3 inflammasome and elevates

IL-1β expression in THP-1 cells

Previous studies have indicated that some viruses interact with immune cells during infection to activate the inflammasome[28, 29]. Considering the central role of inflammation in HCMV associated disorders, we examined the effect of HCMV infection on inflammatory markers in human THP-1 cells. We found that the release of the inflammatory cytokine IL-1β to the culture supernatant was increased in HCMV-infected cells compared with that in control cells (Fig. 3A). Besides, protein levels of NLPR3 and cleaved caspase-1, key components of the inflammasome, were significantly elevated in HCMV-infected cells compared with those in control cells (Fig. 3B-D). Similarly, the mRNA expression of NLPR3 and caspase-1 were also increased in HCMV-infected cells compared with those in control cells (Fig. 3E-F). To test whether NLRP3 is important for HCMV-induced inflammation, THP-1 cells expressing control shRNA (NC) and NLRP3-shRNA were infected with HCMV towne virus. HCMV-induced IL-1β secretion was significantly reduced in NLRP3 knockdown cells compared with NC cells (Fig. 3G-J), suggesting that the inflammasome components NLRP3 is involved in HCMV-induced IL-1β secretion.

Mitochondrial DNA release is required for HCMV induced NLRP3 inflammasome activation

To ensure that mitochondrial dysfunction and mtDNA are needed for NLRP3 inflammasome activation, we measured mtDNA copy number and NLRP3 protein in TFAM knockdown cells. The results showed that TFAM knockdown in THP-1 cells caused an increase in mtDNA copy number in the cytoplasm (Fig. 4A-C), and the

expression level of NLRP3 protein was higher compared with the control group (Fig. 4D-E). These data suggest that TFAM depletion induces mtDNA stress that triggers the release of mtDNA into the cytosol to engage the NLRP3 inflammasome.

To assess the importance of mtDNA in NLRP3 inflammasome activation in HCMV-infected cells, we cultured THP-1 cells with EtBr to generate mtDNA-deficient cells. Low concentrations of EtBr, resulting in inhibition of mtDNA replication, have no detectable effect on nuclear DNA division [30]. We confirmed that EtBr treatment diminished the mtDNA copy number in THP-1 cells (Fig. 4F). The protein levels of NLRP3 and IL-1β were analyzed by Western blotting 48 hours after HCMV infection. The results showed that EtBr treatment inhibited HCMV-induced NLRP3 protein and IL-1β expression (Fig. 4G-I). Together, these results indicate that mtDNA depletion prevented NLRP3 inflammasome activation.

Discussion

HCMV has been reported to cause inflammation, such as apical periodontitis, retinitis, colitis, and neonatal infection [31-35]. The inflammatory responses and cytokines play a key role in HCMV infection, reactivation, and disease progression [36-38]. However, the mechanism behind the activation of inflammation is poorly elucidated. Consequently, our team was committed to this point and the corresponding data indicated that HCMV infection in THP-1 cells could significantly induce the activation of NLRP3 inflammasome, which has not been reported before. Interestingly, Botto, S et al. found that AIM2 but neither IFI16 nor NLRP3 is essential to

HCMV-mediated IL-1β secretion, which is different from our conclusion[39]. In our study, we used the HCMV Towne strain to infect THP-1 cells. These cells were not treated with PMA, which were not differentiated into a macrophage, and thus the virus retained the latent infection in THP-1 cells with a monocyte-like phenotype.

NLRP3 inflammasome is at the central stage of the inflammatory response, regulating the caspase-1 activity to induce proteolytic maturation of IL-1β [40]. Mitochondrion, as an important organelle in the cell, regulates various biological processes such as energy metabolism, innate immune response, and apoptosis, which is essential for maintaining cell homeostasis [41]. The present study provides evidence that mitochondria play a major role in NLRP3 inflammasome signaling [15, 42, 43]. However, the direct impact of HCMV infection on mitochondria in THP-1 cells and whether mitochondria are involved in the NLRP3 inflammasome activation process remain largely unknown.

Previous studies have reported the effects of HCMV on mitochondrial function, but these are mainly related to apoptosis and host cell metabolism [44-46]. We focused on morphological and functional change in mitochondria during HCMV infection. Many viruses have been shown to cause mitochondrial and mtDNA damage [23, 47, 48]. Mitochondria are sources of ROS production [49]. Research suggests that high levels of ROS could lead to loss of ΔΨ, oxidative stress, and DNA damage [50, 51]. Consistent with the results above, we concluded that HCMV infection of THP-1 cells resulted in the accumulation of intracellular ROS, a decrease of mitochondrial membrane potential, mitochondrial DNA damage, and release into the cytosol. HCMV infection

causes mitochondrial dysfunction in THP-1 cells.

To further investigate the impact of HCMV on mitochondria, we further observed mitochondria by electron microscopy and fluorescence confocal microscopy. The corresponding results showed that HCMV infection caused a change in mitochondrial morphology and dynamics. At the molecular level, we also found that HCMV-infection resulted in increased expression of mitochondrial fusion proteins MFN1, OPA1, and OMA1. Mitochondrial morphology depends on an appropriate balance between fusion and fission processes [14]. Mitochondrial morphology change may be related to disturbances in mitochondrial function [52]. The fusion of mitochondria is considered as a rescue mechanism for damaged organelles [53]. We think that the fusion of mitochondria is a rescue mechanism for damaged organelles to prevent host cell apoptosis [53].

These results demonstrate that HCMV infection leads to mitochondrial dysfunction and mtDNA release into the cytosol ultimately. It has been reported that injection of mtDNA into mouse joints will induce arthritis exposure of spleen cells to mtDNA will increase the secretion of pro-inflammatory cytokines [54]. Previous studies also showed that mtDNA stress primes the antiviral innate immune response [55]. We hypothesized that NLRP3 inflammasome activation might be connected to mtDNA release after HCMV infection of THP-1 cells.

TFAM plays a significant role in the replication, transcription, and maintenance of mtDNA [56]. We found that the TFAM depletion and the release of mtDNA were significantly increased after HCMV infection, which is a common phenomenon of

herpes virus infection but not a general consequence of viral infection. Cells infected with VSV, Influenza, LCMV, and Vaccinia possessed normal mtDNA architecture, TFAM expression, and copy number [55]. The detailed mechanism still needs further study. Next, we thought to determine whether HCMV-induced mtDNA release is necessary and sufficient to potentiate NLRP3 inflammasome activation. Experimental results show that TFAM knockdown reduced mtDNA contents, leading to the release of mtDNA into the cytoplasm and activation of NLRP3 inflammasome. Furthermore, we found that low-dose EtBr treatment, which can deplete mtDNA in THP-1 cells, inhibits NLRP3 inflammasome activation. As mentioned above, there are reasons to think that mtDNA causes the activation of NLRP3 inflammasome**.**

Conclusions

In this study, we found HCMV infection dramatically induced the activation of NLRP3 inflammasome. Simultaneously, except for the HCMV-medicated NLRP3 signaling activation mentioned above, our evidence suggests that mitochondrial dysfunction can enhance ROS generation, and mtDNA release may contribute to the NLRP3 activation as well.

Methods

Cell culture and virus infections

THP-1 cells cultured in RPMI 1640 medium (Life Technologies, Grand Island, NY) supplemented with 10% fetal bovine serum (FBS, Life Technologies, Grand Island, NY) and antibiotics (100 units/ ml penicillin and 100 μg/ml streptomycin)

were obtained from the cell bank of the Shanghai Institute, and maintained in RPMI-1640 medium (Gibco) with 10% FBS, 100 U/ml penicillin and 100 μg/ml streptomycin. THP-1 cells were nfected with HCMV Towne strain as a previous description [57]. The Towne strain of HCMV (HCMV-Townevar ATCC), obtained from American Type Culture Collection (ATCC), was a gift from Dr. Shiqiang Shang (Zhejiang University). HCMV Towne strain was purified by sedimentation through a sucrose gradient, and the infectious virus titers were expressed as median tissue culture infectious dose (TCID50) [58]. Briefly, HF monolayers were infected with CMV virus (MOI of 5) and harvested at 5 dpi (days post-infection). The medium was clarified by low-speed centrifugation (2000 g, 10 min), and virus particles were pelleted (~20000 g, 1 h). Virions were purified on a 15–50% sucrose gradient in phosphate buffer (40 mM mono-/dibasic phosphate, 150 mM NaCl, pH 7.4) using ultracentrifugation (SW 32Ti rotor, Beckman L-90 ultracentrifuge, 24000 rpm, 1 h). Virions were harvested by puncturing the sides of the centrifuge tube with a 23 G needle and were washed once in phosphate buffer before concentrating by centrifugation (SW-41 rotor, Beckman L-80 ultracentrifuge, 24000 rpm, 1 h). The concentration of sucrose in the preparation was reduced by brief dialysis against PBS. A THP-1 cell line was infected with HCMV Towne at a multiplicity of infection (MOI) of 5 and collected at the indicated time points.

Antibodies and reagents

Immunoblot analysis was done using various primary antibodies: anti-NLRP3 antibody (Cell Signaling Technology), anti-AIM2 antibody (Cell Signaling

Technology), anti-ASC antibody (Cell Signaling Technology), anti-Cleaved Caspase-1 antibody (Cell Signaling Technology), anti-TFAM antibody (Abcam), anti-MFN1 antibody (Abcam), anti-OPA1 antibody (Abcam), anti-OMA1 antibody (Abcam), anti-DRP1 antibody (Abcam), anti-Tom20 antibody (Cell Signaling Technology) and anti-GAPDH (Cell Signaling Technology). BCA Protein Assay Kit and Pierce ECL Western Blotting Substrate were obtained from Thermo Scientific (Waltham, MA).

Western blotting

Cells were lysed in RIPA lysis buffer supplemented with protease and phosphatase inhibitors on ice for 20 min, followed by centrifugation at 14,000 rpm for 20 min at 4°C the supernatants were collected. Protein concentrations of whole-cell extracts were determined using the Pierce BCA protein assay kit. Lysates with the same concentration of protein were loaded in 10% SDS-PAGE gels, followed by electrophoretic transferred onto nitrocellulose membranes. Then membranes were blocked for 1 hour at room temperature in 5% non-fat milk in Tris-buffered saline (TBS)-Tween (TBS-T) on a shaker and then incubated with the primary antibodies overnight at 4°C. The membrane was washed three times with TBST solution for 10 min, following incubation with horseradish peroxidase (HRP) - conjugated anti-rabbit or anti-mouse immunoglobulin G at room temperature for 1 hour with gentle shaking. Immunoreactive proteins were detected by ECL reagent according to the manufacturer's protocol (Thermo Scientific, Rockford, IL). Optical density was measured using the National Institute of Health Image J software. Relative protein

levels were normalized to the GAPDH level in samples.

ELISA

Cell debris was centrifuged and removed, which the resulting supernatant was collected. Concentrations of human IL-1β from the cell culture supernatant were determined by ELISA kits (Dakewe Biotech, China) according to the instructions provided by the company.

Real-time PCR

Cells were harvested and lysates prepared. The total RNA was isolated from cells with the help of Trizol (Invitrogen) according to the manufacturer's protocol. Equal amounts of RNA were reverse-transcribed into cDNA using the Reverse Transcription Kit (Takara). The complementary cDNA was subsequently used as a template for real-time PCR. Real-time quantitative PCR analysis was performed using 3 μl cDNA /20 μl reaction volume on a CFX Connect™ Real-Time PCR Detection System (Bio-Rad, Hercules, CA) using SYBR Green according to the manufacturer's instructions. PCR conditions were 95˚C for 2 min, 95˚C for 15 s, and 60˚C for 30 s for 40 cycles. Three technical replicates were performed for each biological sample, and expression values of each replicate were normalized against GAPDH cDNA using the $2^{-\Delta\Delta Ct}$ method.

For mitochondrial DNA (mtDNA) copy number detection, cell pellets were divided into two parts to extract total DNA and cytosolic DNA, respectively. Cytosolic DNA was isolated from the pure cytosolic fractions using the TIAamp Genomic DNA kit (TIAamp, China). Total DNA was extracted directly from the same

kit. Quantitative PCR was used for the measurement of mtDNA using established primers for mitochondrial and nuclear genes. The relative abundance of mtDNA was normalized to that of nuclear DNA as the ratio of mitochondrial DNA encoded genes (COX2, ND1, DloopHV1) to nuclear DNA encoding 18S ribosomal RNA.

The primer sets used for RT-PCR are listed in Table 1.

Lentivirus production and transduction

Hairpin-pLKO.1 vectors (carrying a puromycin antibiotic resistance gene) containing control and TFAM-shRNA oligonucleotides were purchased from Biogot Technology (Nanjing, China). Sequences of specific shRNAs used in this study were as follows: shTFAM 5' GGCAAGTTGTCCAAAGAAACC3' (forward); Lentiviral production and transduction were conducted according to manufacturer's protocol (GeneCopoeia, Rockville, MD). TFAM knockdown in THP-1 cells was validated by western blot analysis.

ROS detection

ROS level in THP-1 cells was assessed by measuring the fluorescence of 2′,7′-dichlorofluorescin diacetate (DCFH-DA), an oxidation sensitive probe, according to the manufacturer's protocol (Beyotime, Shanghai, China). Briefly, DCFH-DA (10 μM) was added to the THP-1 cells for 20 min at 37 ℃. Labeled cells were washed twice in modified PBS before analyzed by a confocal microscope (Olympus, Fluoview1000, Tokyo, Japan). Relative ROS levels were presented as fluorescence intensity.

Mitochondrial membrane potential (Δψm) measurement

The mitochondrial membrane potential was tested using a JC-1 assay kit (JC-1 assay kit, Beyotime, Shanghai, China) according to the manufacturer's instructions. The cells were washed twice with PBS and incubated with JC-1 probe at 37 °C in the dark incubator for 30 min. After washing, green and red fluorescent intensity was analyzed by confocal microscopy. The Δψm was calculated as the fluorescence intensity ratio of green to the total.

Fluorescent confocal microscopy

The cells were mixed with Mito-Tracker Red (Invitrogen) and placed in the incubator at 37 °C for 30 minutes in the dark according to the manufacturer's recommended protocol. The cells were washed in PBS, then 200 ul of 4% paraformaldehyde was added to the cell pellet, mixed, and left at room temperature for 10 min to 15 min, permeabilized with 0.5% Triton X-100 for 15 min, and then stained with DAPI for 20 min. Cells were washed with PBS between two steps. Cells were spun onto the slide and sealed with an anti-fluorescence quencher. Images were obtained using Nikon A1 confocal microscope.

Cells are classified by measuring the length-to-width ratio of mitochondria. More than 50% of mitochondria in a cell show that the length-to-width ratio of more than 20 is defined as the network type. More than 50% of mitochondria in one-cell show that the length-to-width ratio is less than 20 is defined as the fragment type [59].

Electron microscopy

The THP-1 cells were collected, washed 3 times with pre-cooled PBS, and then fixed in 2.5% glutaric acid for 2 h at 4 °C. Next, the cells were fixed using 1% osmic

acid for 2 hours at 4 °C and dehydration of gradient ethanol was used at 4 °C. Cells were washed with pre-cooled PBS between each step. After embedded, the cells were sliced and stained with lead citrate. The intracellular mitochondrial morphology was observed and photographed by transmission electron microscopy. The mitochondrial perimeter of the mock and infected cells was measured by Image J software [55]. Count the number of mitochondria with a circumference of fewer than 2 μm, 2 to 5 μm, and greater than 5 μm, and calculate the percentage of each.

Generation of mtDNA-deficient cells

THP-1 cells were cultured in RPMI 1640 medium (Life Technologies, Grand Island, NY) containing 10% fetal bovine serum (FBS, Life Technologies, Grand Island, NY), antibiotics (100 units/ ml penicillin and 100 μg/ml streptomycin) at 37 °C in an atmosphere of 5% CO2. Cells were incubated in the medium supplemented with 100 μg/ml pyruvate (Invitrogen), 50 μg/ml uridine (Sigma) and ethidium bromide (EtBr) (25 ng/ml) for 2 weeks [15, 60]. Quantitative real-time PCR was used to determine the depletion of mitochondrial DNA.

Statistical analysis

Unpaired t-tests were used to compare other data between mock and HCMV-infected samples. All statistical values were visualized using GraphPad Prism 5.0. $p \leq 0.05$ was considered to be statistically signifcant.

All methods were carried out in accordance with relevant guidelines and regulations.

Abbreviations

HCMV: Human Cytomegalovirus; IL-1β: interleukin-1β; NLRP3: NLR family pyrin domain containing 3; ROS: reactive oxygen species; ΔΨm: mitochondrial membrane potential; EtBr: ethidium bromide; TFAM: transcription factor A, mitochondrial.

Declarations

Compliance with Ethics Guidelines

This article does not contain any studies with human or animal subjects performed by any of the authors.

Ethics approval and consent to participate

Not applicable.

Consent for publication

Not applicable.

Availability of data and materials

All the data and materials used in this report are included in the manuscript.

Conflict of interest

The authors declared that they have no competing interest.

Acknowledgments

We thank Haihua Gu and members of the Zheng lab for their suggestions on this manuscript.

Funding

Science and Technology Planning Project of Wenzhou, Zhejiang, China (No. Y20180108); Science and Technology Planning Project of Zhejiang Province, China

(No. 2018C37067); Natural Science Foundation of Zhejiang Province, China (No. LY18H200006).

Data and materials statement

The datasets used and/or analysed during the current study are available from the corresponding author on reasonable request.

Authors' contributions

All authors participated in the design, interpretation of the studies, and analysis of the data and review of the manuscript; Conceptualization: Xiaoqun Zheng; Methodology :Linhua Lan; Formal analysis and investigation: Meimei Lai. Qiongdan Wang; Writing - original draft preparation: Yutian Lu; Writing - review and editing: Xi Xu; Funding acquisition: Binhan Guo; Resources: Kaizhao Huang; Supervision:Ying Peng.

References

[1] TAYLOR-WIEDEMAN J, SISSONS J G, BORYSIEWICZ L K, et al. Monocytes are a major site of persistence of human cytomegalovirus in peripheral blood mononuclear cells [J]. The Journal of general virology, 1991, 72 (Pt 9)(2059-64.

[2] LEE J H, KALEJTA R F. Human Cytomegalovirus Enters the Primary CD34+ Hematopoietic Progenitor Cells where it Establishes Latency by Macropinocytosis [J]. Journal of virology, 2019,

[3] JIA Y J, LIU J, HAN F F, et al. Cytomegalovirus infection and atherosclerosis risk: A meta-analysis [J]. Journal of medical virology, 2017, 89(12): 2196-206.

[4] LV Y L, HAN F F, JIA Y J, et al. Is cytomegalovirus infection related to inflammatory bowel disease, especially steroid-resistant inflammatory bowel disease? A meta-analysis [J]. Infection and drug resistance, 2017, 10(511-9.

[5] RAHBAR A, BOSTROM L, LAGERSTEDT U, et al. Evidence of active cytomegalovirus infection and increased production of IL-6 in tissue specimens obtained from patients with inflammatory bowel diseases [J]. Inflammatory bowel diseases, 2003, 9(3): 154-61.

[6] SELEME M C, KOSMAC K, JONJIC S, et al. Tumor Necrosis Factor Alpha-Induced Recruitment of Inflammatory Mononuclear Cells Leads to Inflammation and Altered Brain Development in Murine Cytomegalovirus-Infected Newborn Mice [J]. J Virol, 2017, 91(8):

[7] IWASAKI A, MEDZHITOV R. Control of adaptive immunity by the innate immune system [J]. Nature immunology, 2015, 16(4): 343-53.

[8] MARTINON F, BURNS K, TSCHOPP J. The inflammasome: a molecular platform triggering activation of inflammatory caspases and processing of proIL-beta [J]. Molecular cell, 2002, 10(2): 417-26.
[9] TORII Y, KAWADA J I, MURATA T, et al. Epstein-Barr virus infection-induced inflammasome activation in human monocytes [J]. PloS one, 2017, 12(4): e0175053.
[10] HALFMANN P, HILL-BATORSKI L, KAWAOKA Y. The Induction of IL-1beta Secretion Through the NLRP3 Inflammasome During Ebola Virus Infection [J]. The Journal of infectious diseases, 2018, 218(suppl_5): S504-S7.
[11] ICHINOHE T, PANG I K, IWASAKI A. Influenza virus activates inflammasomes via its intracellular M2 ion channel [J]. Nature immunology, 2010, 11(5): 404-10.
[12] LIU X, COOPER D E, CLUNTUN A A, et al. Acetate Production from Glucose and Coupling to Mitochondrial Metabolism in Mammals [J]. Cell, 2018, 175(2): 502-13 e13.
[13] WEST A P, SHADEL G S, GHOSH S. Mitochondria in innate immune responses [J]. Nature reviews Immunology, 2011, 11(6): 389-402.
[14] CHAN D C. Mitochondria: dynamic organelles in disease, aging, and development [J]. Cell, 2006, 125(7): 1241-52.
[15] NAKAHIRA K, HASPEL J A, RATHINAM V A, et al. Autophagy proteins regulate innate immune responses by inhibiting the release of mitochondrial DNA mediated by the NALP3 inflammasome [J]. Nature immunology, 2011, 12(3): 222-30.
[16] SHIMADA K, CROTHER T R, KARLIN J, et al. Oxidized mitochondrial DNA activates the NLRP3 inflammasome during apoptosis [J]. Immunity, 2012, 36(3): 401-14.
[17] PARK S, WON J H, HWANG I, et al. Defective mitochondrial fission augments NLRP3 inflammasome activation [J]. Scientific reports, 2015, 5(15489.
[18] MARTINON F. Signaling by ROS drives inflammasome activation [J]. European journal of immunology, 2010, 40(3): 616-9.
[19] GOLDMACHER V S. vMIA, a viral inhibitor of apoptosis targeting mitochondria [J]. Biochimie, 2002, 84(2-3): 177-85.
[20] REEVES M B, DAVIES A A, MCSHARRY B P, et al. Complex I binding by a virally encoded RNA regulates mitochondria-induced cell death [J]. Science, 2007, 316(5829): 1345-8.
[21] ZHANG X, WU X, HU Q, et al. Mitochondrial DNA in liver inflammation and oxidative stress [J]. Life sciences, 2019,
[22] KUNKEL G H, KUNKEL C J, OZUNA H, et al. TFAM overexpression reduces pathological cardiac remodeling [J]. Molecular and cellular biochemistry, 2019, 454(1-2): 139-52.
[23] CYMERYS J, CHODKOWSKI M, SLONSKA A, et al. Disturbances of mitochondrial dynamics in cultured neurons infected with human herpesvirus type 1 and type 2 [J]. Journal of neurovirology, 2019,
[24] MAURICE N M, BEDI B, YUAN Z, et al. Pseudomonas aeruginosa Induced Host Epithelial Cell Mitochondrial Dysfunction [J]. Scientific reports, 2019, 9(1): 11929.
[25] WESTERMANN B. Molecular machinery of mitochondrial fusion and fission [J]. The Journal of biological chemistry, 2008, 283(20): 13501-5.
[26] CIPOLAT S, MARTINS DE BRITO O, DAL ZILIO B, et al. OPA1 requires mitofusin 1 to promote mitochondrial fusion [J]. Proceedings of the National Academy of Sciences of the United States of America, 2004, 101(45): 15927-32.
[27] VAN DER BLIEK A M, SHEN Q, KAWAJIRI S. Mechanisms of mitochondrial fission and fusion [J]. Cold Spring Harbor perspectives in biology, 2013, 5(6):
[28] RAJAN J V, RODRIGUEZ D, MIAO E A, et al. The NLRP3 inflammasome detects

encephalomyocarditis virus and vesicular stomatitis virus infection [J]. Journal of virology, 2011, 85(9): 4167-72.
[29] INDALAO I L, SAWABUCHI T, TAKAHASHI E, et al. IL-1beta is a key cytokine that induces trypsin upregulation in the influenza virus-cytokine-trypsin cycle [J]. Archives of virology, 2017, 162(1): 201-11.
[30] KENNEDY E D, MAECHLER P, WOLLHEIM C B. Effects of depletion of mitochondrial DNA in metabolism secretion coupling in INS-1 cells [J]. Diabetes, 1998, 47(3): 374-80.
[31] JAKOVLJEVIC A, KNEZEVIC A, NIKOLIC N, et al. Herpesviruses viral loads and levels of proinflammatory cytokines in apical periodontitis [J]. Oral diseases, 2018, 24(5): 840-6.
[32] ALSTON C I, DIX R D. SOCS and Herpesviruses, With Emphasis on Cytomegalovirus Retinitis [J]. Frontiers in immunology, 2019, 10(732.
[33] CICCOCIOPPO R, RACCA F, PAOLUCCI S, et al. Human cytomegalovirus and Epstein-Barr virus infection in inflammatory bowel disease: need for mucosal viral load measurement [J]. World journal of gastroenterology, 2015, 21(6): 1915-26.
[34] NELSON C S, HEROLD B C, PERMAR S R. A new era in cytomegalovirus vaccinology: considerations for rational design of next-generation vaccines to prevent congenital cytomegalovirus infection [J]. NPJ vaccines, 2018, 3(38.
[35] SODERBERG-NAUCLER C. Does cytomegalovirus play a causative role in the development of various inflammatory diseases and cancer? [J]. Journal of internal medicine, 2006, 259(3): 219-46.
[36] NABEKURA T, LANIER L L. Tracking the fate of antigen-specific versus cytokine-activated natural killer cells after cytomegalovirus infection [J]. The Journal of experimental medicine, 2016, 213(12): 2745-58.
[37] BIRON C A, TARRIO M L. Immunoregulatory cytokine networks: 60 years of learning from murine cytomegalovirus [J]. Medical microbiology and immunology, 2015, 204(3): 345-54.
[38] CLEMENT M, HUMPHREYS I R. Cytokine-Mediated Induction and Regulation of Tissue Damage During Cytomegalovirus Infection [J]. Frontiers in immunology, 2019, 10(78.
[39] BOTTO S, ABRAHAM J, MIZUNO N, et al. Human Cytomegalovirus Immediate Early 86-kDa Protein Blocks Transcription and Induces Degradation of the Immature Interleukin-1beta Protein during Virion-Mediated Activation of the AIM2 Inflammasome [J]. mBio, 2019, 10(1):
[40] BROZ P, DIXIT V M. Inflammasomes: mechanism of assembly, regulation and signalling [J]. Nature reviews Immunology, 2016, 16(7): 407-20.
[41] BRATIC I, TRIFUNOVIC A. Mitochondrial energy metabolism and ageing [J]. Biochimica et biophysica acta, 2010, 1797(6-7): 961-7.
[42] MOHANTY A, TIWARI-PANDEY R, PANDEY N R. Mitochondria: the indispensable players in innate immunity and guardians of the inflammatory response [J]. Journal of cell communication and signaling, 2019,
[43] ZHOU R, YAZDI A S, MENU P, et al. A role for mitochondria in NLRP3 inflammasome activation [J]. Nature, 2011, 469(7329): 221-5.
[44] LEWIS R A, WATKINS L, ST JEOR S. Enhancement of deoxyguanosine kinase activity in human lung fibroblast cells infected with human cytomegalovirus [J]. Molecular and cellular biochemistry, 1984, 65(1): 67-71.
[45] VYSOCHAN A, SENGUPTA A, WELJIE A M, et al. ACSS2-mediated acetyl-CoA synthesis from acetate is necessary for human cytomegalovirus infection [J]. Proceedings of the National Academy of Sciences of the United States of America, 2017, 114(8): E1528-E35.

[46] GYU-CHEOL L, LEE J H, KIM B Y, et al. Mitochondria-Targeted Apoptosis in Human Cytomegalovirus-Infected Cells [J]. J Microbiol Biotechn, 2013, 23(11): 1627-35.
[47] LI Y, YANG D, JIA Y, et al. Effect of infectious bursal disease virus infection on energy metabolism in embryonic chicken livers [J]. British poultry science, 2019, 1-7.
[48] WIEDMER A, WANG P, ZHOU J, et al. Epstein-Barr virus immediate-early protein Zta co-opts mitochondrial single-stranded DNA binding protein to promote viral and inhibit mitochondrial DNA replication [J]. Journal of virology, 2008, 82(9): 4647-55.
[49] MAILLOUX R J, JIN X, WILLMORE W G. Redox regulation of mitochondrial function with emphasis on cysteine oxidation reactions [J]. Redox biology, 2014, 2(123-39.
[50] YAN S, SORRELL M, BERMAN Z. Functional interplay between ATM/ATR-mediated DNA damage response and DNA repair pathways in oxidative stress [J]. Cellular and molecular life sciences : CMLS, 2014, 71(20): 3951-67.
[51] ZOROV D B, JUHASZOVA M, SOLLOTT S J. Mitochondrial reactive oxygen species (ROS) and ROS-induced ROS release [J]. Physiological reviews, 2014, 94(3): 909-50.
[52] PICARD M, SHIRIHAI O S, GENTIL B J, et al. Mitochondrial morphology transitions and functions: implications for retrograde signaling? [J]. American journal of physiology Regulatory, integrative and comparative physiology, 2013, 304(6): R393-406.
[53] NI H M, WILLIAMS J A, DING W X. Mitochondrial dynamics and mitochondrial quality control [J]. Redox biology, 2015, 4(6-13.
[54] COLLINS L V, HAJIZADEH S, HOLME E, et al. Endogenously oxidized mitochondrial DNA induces in vivo and in vitro inflammatory responses [J]. Journal of leukocyte biology, 2004, 75(6): 995-1000.
[55] WEST A P, KHOURY-HANOLD W, STARON M, et al. Mitochondrial DNA stress primes the antiviral innate immune response [J]. Nature, 2015, 520(7548): 553-7.
[56] KAUFMAN B A, DURISIC N, MATIVETSKY J M, et al. The mitochondrial transcription factor TFAM coordinates the assembly of multiple DNA molecules into nucleoid-like structures [J]. Molecular biology of the cell, 2007, 18(9): 3225-36.
[57] ZHENG X, GAO Y, ZHANG Q, et al. Identification of transcription factor AML-1 binding site upstream of human cytomegalovirus UL111A gene [J]. PloS one, 2015, 10(2): e0117773.
[58] BRITT W J. Human cytomegalovirus: propagation, quantification, and storage [J]. Current protocols in microbiology, 2010, Chapter 14(Unit 14E 3.
[59] WANG H, YI J, LI X, et al. ALS-associated mutation SOD1(G93A) leads to abnormal mitochondrial dynamics in osteocytes [J]. Bone, 2018, 106(126-38.
[60] HASHIGUCHI K, ZHANG-AKIYAMA Q M. Establishment of human cell lines lacking mitochondrial DNA [J]. Methods in molecular biology, 2009, 554(383-91.

Fig.1 HCMV infection causes mitochondrial dysfunction and mtDNA releasing into cytosol in THP-1 cells.

a The levels of HCMV transcripts (IE1, LUNA, and UL83 mRNA) in latent infection analyzed by RT-PCR. **b** ROS levels in mitochondria of THP-1 cells infected with HCMV (MOI=5) for 48 h. Uninfected cells serve as mock control. **c**Mitochondrial membrane potential in THP-1 cells infected with HCMV (MOI=5) for 48 h. Uninfected cells serve as mock control. **d,e** Immunoblot analysis of TFAM in lysates from control and THP-1 cells infected with HCMV (MOI=5) for 48 h. GAPDH was used as loading control. **f** Relative qRT–PCR analysis of TFAM mRNA level in THP-1 cells infected with HCMV (MOI=5) for 48 h. **g** Relative mtDNA copy number of THP-1 cells 48 h post-infection with HCMV (MOI=5). **h** Cytosolic mtDNA was quantitated via qPCR. Normalization was performed as described in the Methods. Data are shown as the mean +/- SEM of three independent experiments. *$p<0.05$, **$p<0.01$, ***$p<0.001$.

Fig.2 HCMV infection interrupts mitochondrial dynamics in THP-1 cells.

a THP-1 cells were infected with HCMV (MOI=5), incubated for the indicated times. Uninfected cells serve as mock control. Cells were fixed and processed for electron microscopy analysis. Blue arrow indicates normal mitochondria, red arrow indicates abnormal of mitochondria. **b** THP-1 cells were infected with HCMV (MOI=5) for the

indicated times. Cells were stained and subjected to confocal microscopy. **c** Mitochondrial perimeter measurements were obtained from multiple independent images, stratified into groups, and graphed as a percentage of the total number of mitochondria counted for each sample. **d** Population of the THP-1 cells with different types of mitochondria morphology was summarized. **e** Immunoblot analysis of MFN1,OPA1,OMA1 and DRP1 in THP-1 cells infected with HCMV (MOI=5) for the indicated time points. GAPDH was used as loading control. Tom20 was used as mitochondrial mass control. **f-h** Quantitative analysis of relative protein levels of MFN1,OPA1,OMA1. Data are shown as the mean +/- SEM of three independent experiments. **p<0.01, ***p<0.001.

Fig.3 HCMV infection significantly activates NLRP3 inflammasome and elevates IL-1β expression in THP-1 cells.

a ELISA of IL-1β in the supernatants of THP-1 cells infected with HCMV (MOI=5) for the indicated time points. **b** Immunoblot analysis of NLPR3 and cleaved caspase-1 in mock and THP-1 cells infected with HCMV (MOI=5) for the indicated time points. **c,d** Quantitative analysis of relative protein levels of NLPR3 and cleaved caspase-1. **e,f** Relative qRT–PCR analysis of NLPR3 and caspase-1 mRNA level in THP-1 cells infected with HCMV (MOI=5) for the indicated time points.

g Immunoblot analysis of NLRP3 in lysates from control and TFAM stable knockdown THP-1 cells. **h** Quantitative analysis of the relative protein levels of NLRP3 in control and TFAM stable knockdown THP-1 cells. **i** Immunoblot analysis

of IL-1β in THP-1 cells infected by HCMV (MOI=5) for 48 h. **j** Quantitative analysis of the relative protein levels of IL-1βin THP-1 cells infected by HCMV (MOI=5) for 48 h. Data are shown as the mean +/- SEM of three independent experiments. *p<0.05, **p<0.01, ***p<0.001.

Fig.4 Mitochondrial DNA release is required for HCMV induced NLRP3 inflammasome activation.

a Immunoblot analysis of TFAM in lysates from control and TFAM stable knockdown THP-1 cells. **b** Quantitative analysis of the relative protein levels of TFAM in control and TFAM stable knockdown THP-1 cells. **c** Cytosolic mtDNA was quantitated by qPCR in TFAM stable knockdown THP-1 cells. **d** Immunoblot analysis of NLRP3 in TFAM stable knockdown THP-1 cells. **e** Quantitative analysis of the relative protein levels of NLRP3 in control and TFAM stable knockdown THP-1 cells. **f** mtDNA abundance of THP-1 cells treated with (25 ng / ml) EtBr for 2 weeks. **g** Immunoblot analysis of NLRP3 and IL-1β in THP-1 cells treated with or without EtBr followed by HCMV infection (MOI=5) for 48 h. **h** Quantitative analysis of the relative protein levels of NLRP3 in THP-1 cells treated with or without EtBr followed by HCMV infection (MOI=5) for 48 h. **i** Quantitative analysis of the relative protein levels of IL-1β in THP-1 cells treated with or without EtBr followed by HCMV infection (MOI=5) for 48 h. Data are shown as the mean +/- SEM of three independent experiments. *p<0.05, **p<0.01, ***p<0.001. NS (non-significant).

Table 1. Primers used for RT-PCR amplification.

Primer name	Nucleotide sequence (5' to 3)	Product size(bp)
TFAM forward	GAAGCTAAGGGTGATTCACCGC	182
TFAM reverse	CGTAGAAGATCCTTTCGTCCAAC	
GAPDH forward	CTGCACCACCAACTGCTTAG	185
GAPDH revers	GAGGTCCACCACTGACACGTT	
NLRP3 forward	TGGAGACACAGGACTCAGGC	252
NLRP3 reverse	CATTTCACCCAACTGTAGGC	
Caspase-1 forward	GCAAAGCTTGACATTCCCTT	220
Caspase-1 reverse	GCAAAGCTTGACATTCCCTT	
COX2 forward	CCCCACATTAGGCTTAAAAACAGAT	81
COX2 reverse	TATACCCCCGGTCGTGTAGC	
ND1 forward	CCTAATGCTTACCGAACGA	152
ND1 reverse	GGGTGATGGTAGATGTGGC	
DloopHV1 forward	CGGTACCATAAATACTTGACCAC	123
DloopHV1 reverse	GAGTTGCAGTTGATGTGTGATAG	
18S forward	CGACCCATTCGAACGTCTG	116
18S reverse	CCGTTTCTCAGGCTCCCTC	

Figures

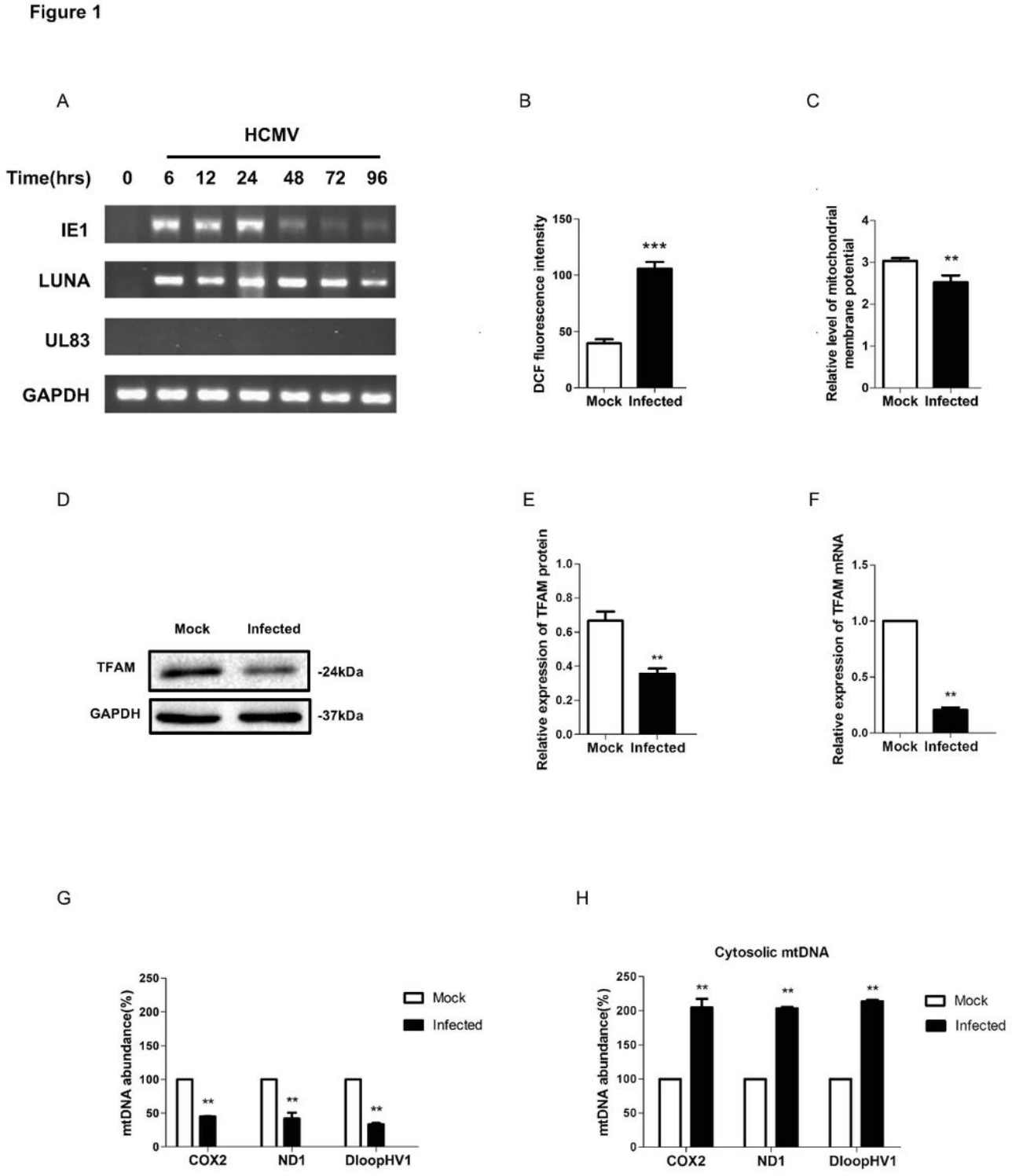

Figure 1

HCMV infection causes mitochondrial dysfunction and mtDNA releasing into cytosol in THP-1 cells.

a The levels of HCMV transcripts (IE1, LUNA, and UL83 mRNA) in latent infection analyzed by RT-PCR. b ROS levels in mitochondria of THP-1 cells infected with HCMV (MOI=5) for 48 h. Uninfected cells serve as mock control. cMitochondrial membrane potential in THP-1 cells infected with HCMV (MOI=5) for 48 h. Uninfected cells serve as mock control. d,e Immunoblot analysis of TFAM in lysates from control and THP-1 cells infected with HCMV (MOI=5) for 48 h. GAPDH was used as loading control. f Relative qRT–PCR analysis of TFAM mRNA level in THP-1 cells infected with HCMV (MOI=5) for 48 h. g Relative mtDNA copy number of THP-1 cells 48 h post-infection with HCMV (MOI=5). h Cytosolic mtDNA was quantitated via qPCR. Normalization was performed as described in the Methods. Data are shown as the mean +/- SEM of three independent experiments. *$p<0.05$, **$p<0.01$, ***$p<0.001$.

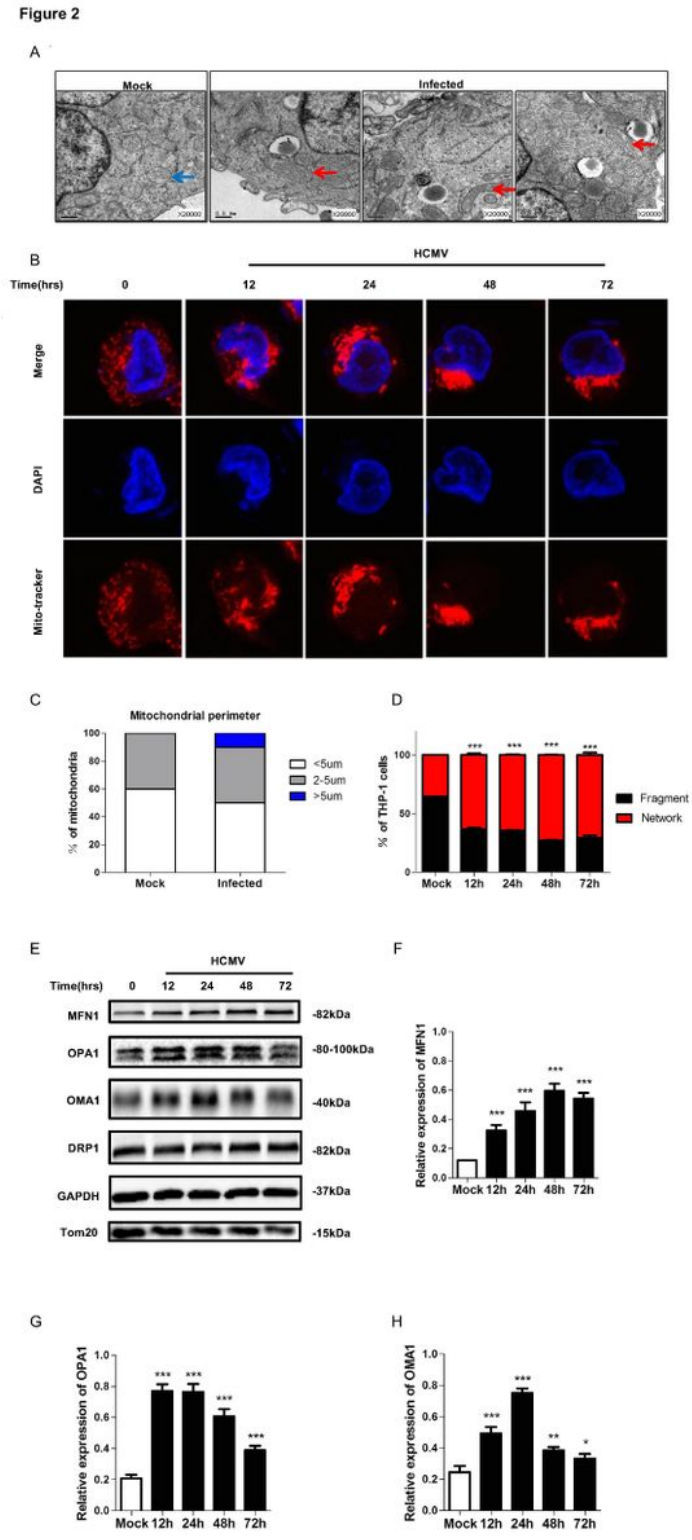

Figure 2

HCMV infection interrupts mitochondrial dynamics in THP-1 cells.

a THP-1 cells were infected with HCMV (MOI=5), incubated for the indicated times.

Uninfected cells serve as mock control. Cells were fixed and processed for electron

microscopy analysis. Blue arrow indicates normal mitochondria, red arrow indicates abnormal of mitochondria. b THP-1 cells were infected with HCMV (MOI=5) for the indicated times. Cells were stained and subjected to confocal microscopy. c Mitochondrial perimeter measurements were obtained from multiple independent images, stratified into groups, and graphed as a percentage of the total number of mitochondria counted for each sample. d Population of the THP-1 cells with different types of mitochondria morphology was summarized. e Immunoblot analysis of MFN1,OPA1,OMA1 and DRP1 in THP-1 cells infected with HCMV (MOI=5) for the indicated time points. GAPDH was used as loading control. Tom20 was used as mitochondrial mass control. f-h Quantitative analysis of relative protein levels of MFN1,OPA1,OMA1. Data are shown as the mean +/- SEM of three independent experiments. **p<0.01, ***p<0.001.

Figure 3

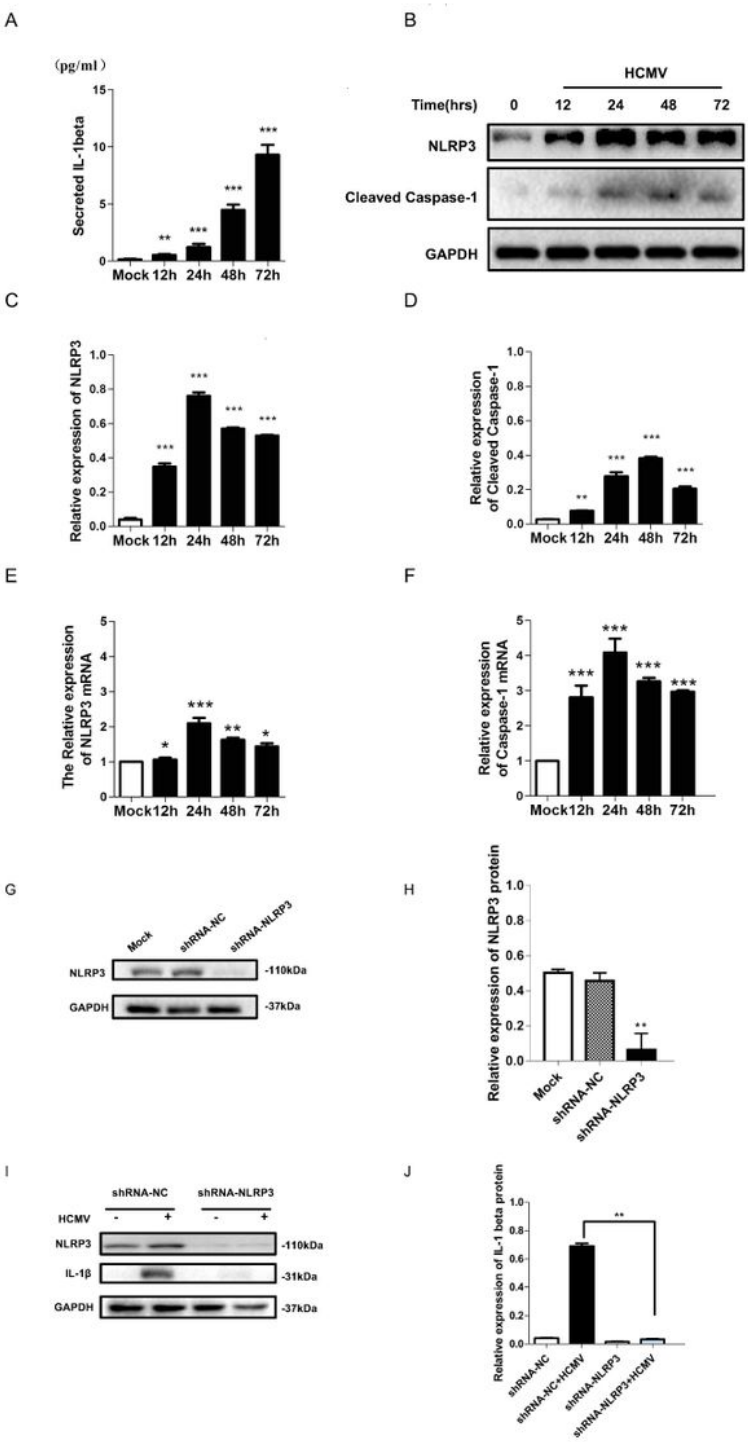

Figure 3

HCMV infection significantly activates NLRP3 inflammasome and elevates

IL-1β expression in THP-1 cells.

a ELISA of IL-1β in the supernatants of THP-1 cells infected with HCMV (MOI=5)

for the indicated time points. b Immunoblot analysis of NLPR3 and cleaved

caspase-1 in mock and THP-1 cells infected with HCMV (MOI=5) for the indicated

time points. c,d Quantitative analysis of relative protein levels of NLPR3 and cleaved

caspase-1. e,f Relative qRT–PCR analysis of NLPR3 and caspase-1 mRNA level in

THP-1 cells infected with HCMV (MOI=5) for the indicated time points.

g Immunoblot analysis of NLRP3 in lysates from control and TFAM stable

knockdown THP-1 cells. h Quantitative analysis of the relative protein levels of

NLRP3 in control and TFAM stable knockdown THP-1 cells. i Immunoblot analysis of IL-1β in THP-1 cells infected by HCMV (MOI=5) for 48 h. j Quantitative analysis

of the relative protein levels of IL-1βin THP-1 cells infected by HCMV (MOI=5) for

48 h. Data are shown as the mean +/- SEM of three independent experiments. *p<0.05, **p<0.01, ***p<0.001.

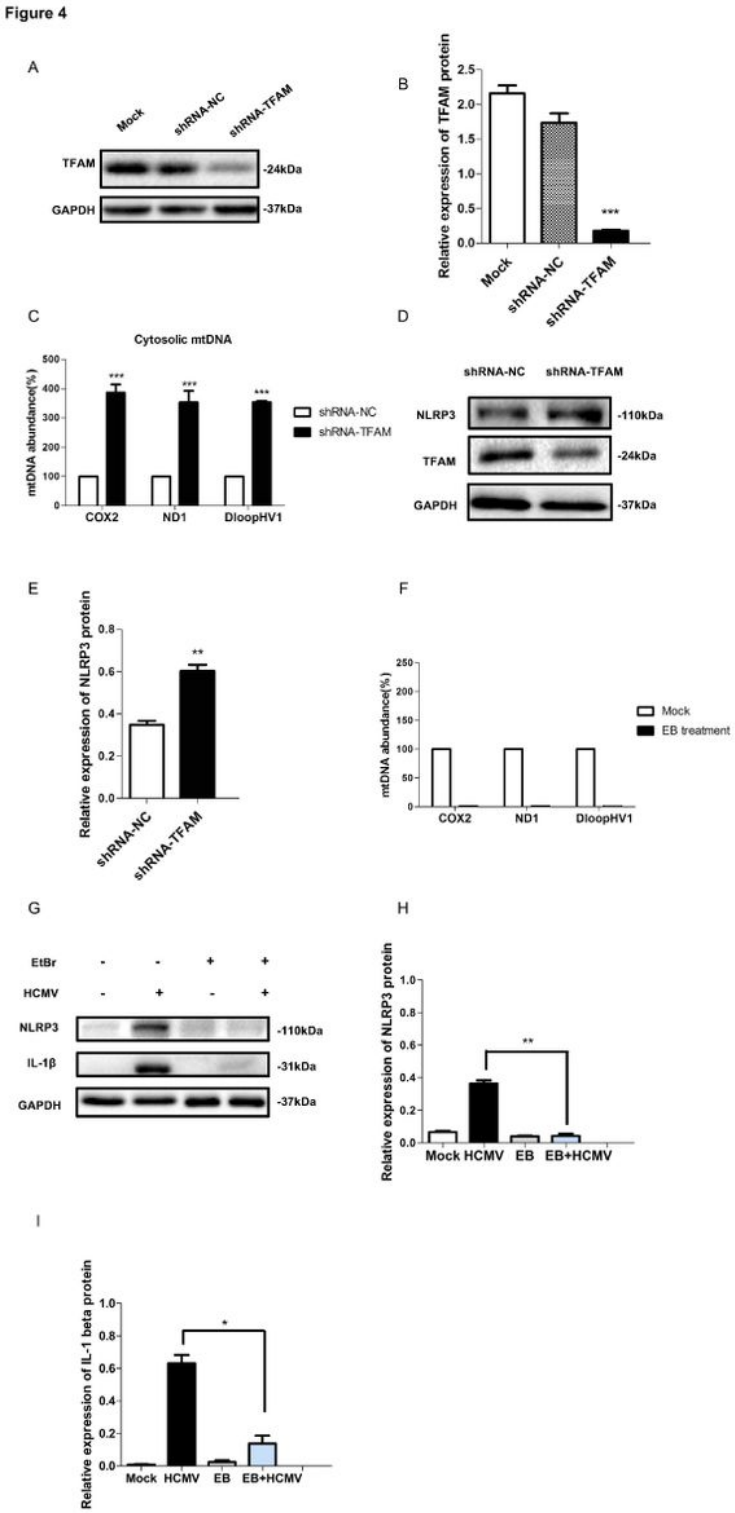

Figure 4

Mitochondrial DNA release is required for HCMV induced NLRP3 inflammasome activation.

a Immunoblot analysis of TFAM in lysates from control and TFAM stable knockdown

THP-1 cells. b Quantitative analysis of the relative protein levels of TFAM in control and TFAM stable knockdown THP-1 cells. c Cytosolic mtDNA was quantitated by qPCR in TFAM stable knockdown THP-1 cells. d Immunoblot analysis of NLRP3 in TFAM stable knockdown THP-1 cells. e Quantitative analysis of the relative protein levels of NLRP3 in control and TFAM stable knockdown THP-1 cells. f mtDNA abundance of THP-1 cells treated with (25 ng / ml) EtBr for 2 weeks. g Immunoblot analysis of NLRP3 and IL-1β in THP-1 cells treated with or without EtBr followed by HCMV infection (MOI=5) for 48 h. h Quantitative analysis of the relative protein levels of NLRP3 in THP-1 cells treated with or without EtBr followed by HCMV infection (MOI=5) for 48 h. i Quantitative analysis of the relative protein levels of IL-1β in THP-1 cells treated with or without EtBr followed by HCMV infection (MOI=5) for 48 h. Data are shown as the mean +/- SEM of three independent experiments. *$p<0.05$, **$p<0.01$, ***$p<0.001$. NS (non-significant).